Laboratory Investigation (2015) 95, 1429–1438

Myofibroblasts contribute to but are not necessary for wound contraction

Mohamed M Ibrahim[1,5], Lei Chen[2,5], Jennifer E Bond[1], Manuel A Medina[1], Licheng Ren[1,3], George Kokosis[1], Angelica M Selim[4] and Howard Levinson[1,4]

Wound contraction facilitates tissue repair. The correct balance between too little contraction, which leads to non-healing wounds, and too much contraction, which leads to contractures, is important for optimal healing. Thus, understanding which cells cause wound contraction is necessary to optimize repair. Wound contraction is hypothesized to develop from myofibroblast (cells which express alpha-smooth muscle actin; ACTA2) contractility, while the role of fibroblast contractility is unknown. In this study, we utilized ACTA2 null mice to determine what role fibroblasts play in wound contraction. Human scar contractures were immunostained for ACTA2, beta-cytoplasmic actin (ACTB), and gamma-cytoplasmic actin (ACTG1). Full-thickness cutaneous wounds were created on dorsum of $ACTA2^{+/+}$ mice and strain-matching $ACTA2^{+/-}$ and $ACTA2^{-/-}$ mice. Wound contraction was quantified. Tissue was harvested for histologic, immunohistochemical and protein analysis. Compared with surrounding unwounded skin, human scar tissue showed increased expression of ACTA2, ACTB, and ACTG1. ACTA2 was focally expressed in clusters. ACTB and ACTG1 were widely, highly expressed throughout scar tissue. Wound contraction was significantly retarded in $ACTA2^{-/-}$ mice, as compared to $ACTA2^{+/+}$ controls. Control mice had increased epithelialization, cell proliferation, and neovascularization. $ACTA2^{-/-}$ mice had lower levels of apoptosis, and fewer total numbers of cells. Smaller amount of collagen deposition and immature collagen organization in $ACTA2^{-/-}$ mice demonstrate that wounds were more immature. These data demonstrate that myofibroblasts contribute to but are not necessary for wound contraction. Mechanisms by which fibroblasts promote wound contraction may include activation of contractile signaling pathways, which promote interaction between non-muscle myosin II and ACTB and ACTG1.

Laboratory Investigation (2015) **95,** 1429–1438; doi:10.1038/labinvest.2015.116; published online 14 September 2015

Wound contraction facilitates tissue repair. The correct balance between too little contraction, which leads to non-healing wounds, and too much contraction, which leads to contractures, is important for optimal healing. Thus, understanding which cells cause wound contraction is necessary to optimize repair. Modified fibroblasts with smooth muscle (SM)-like features, including the expression of alpha-SM actin (ACTA2), were first observed by Gabbiani and colleagues in granulation tissue of healing wounds. This led him to suggest that myofibroblasts promote wound contraction and collagen production.[1,2] Subsequent *in vitro* studies by Hinz *et al* demonstrated that myofibroblasts generate increased contractile force, as compared to fibroblasts, and that the mechanism is related to ACTA2 incorporation into stress fibers and increased focal adhesion size.[3–6] ACTA2 levels were found to associate with a fibroblast's ability to wrinkle a deformable substrate and enhance collagen gel contraction.[7]

The compelling hypothesis that myofibroblasts are essential for wound contraction is balanced by a counter hypothesis that myofibroblasts are not essential for wound contraction. Ehrlich *et al* found that human sacrococcygeal pilonidal sinus wounds contract without a high density of myofibroblasts being present, ACTA2 is absent in free-floating collagen lattice contraction, full thickness excisional wounds in rats are capable of unwounded wound contraction in the absence of myofibroblasts, and prevention of ACTA2 expression in rodents treated with vanadate does not alter wound

[1]Division of Plastic and Reconstructive Surgery, Departments of Surgery and Pathology, Duke University Medical Center, Durham, NC, USA; [2]Department of Burn Surgery, First Affiliated Hospital of Sun Yat-Sen University, Guangzhou, Guangdong, China; [3]Department of Burns and Reconstructive Surgery, Xiangya Hospital, Central South University, Changsha, Hunan, China and [4]Department of Pathology, Duke University Medical Center, Durham, NC, USA
Correspondence: Dr H Levinson, MD, Division of Plastic and Reconstructive Surgery, Departments of Surgery and Pathology, Duke University Medical Center, Durham, NC 27710, USA.
E-mail: howard.levinson@duke.edu
[5]These authors contributed equally to this work.

Received 13 January 2015; revised 1 July 2015; accepted 28 July 2015

contraction.[8–12] In 2002, Wrobel *et al*[13] demonstrated that fibroblasts and myofibroblasts produce similar contractile forces.

To determine the role of ACTA2 in wound contraction, we used human scar tissue, Acta2 null ($Acta2^{-/-}$) mice and murine open wound contraction model.[14] Human tissue was immunostained for ACTA2, beta-cytoplasmic actin (ACTB), and gamma-cytoplasmic actin (ACTG1). Human scar tissue showed increased expression of ACTA2, ACTB, and ACTG1. ACTA2 was focally expressed in clusters. ACTB and ACTG1 were widely, highly expressed throughout scar tissue. Wound contraction was significantly retarded in $ACTA2^{-/-}$ mice, as compared to $ACTA2^{+/+}$ controls. Control mice had increased epithelialization, cell proliferation, and neovascularization. $ACTA2^{-/-}$ mice had lower levels of apoptosis, and fewer total numbers of cells. The smaller amount of collagen deposition and immature collagen organization in $ACTA2^{-/-}$ mice demonstrate that the wounds were more immature. We conclude that the expression of ACTA2 is beneficial but not essential for wound contraction.

MATERIALS AND METHODS

Human Tissue

A total of 18 human scar samples with surrounding unwounded tissue were obtained following approved IRB protocols: 12 samples were obtained from First Affiliated Hospital of Sun Yat-sen University in accordance with IRB protocol, and 6 samples were obtained from Duke University Medical Center (DUMC) Department of Pathology. Samples were collected within 1 year of cicatrization. All the included samples exhibited obvious contracture (Supplementary Figure 1). Samples were categorized according to patients' race, gender, age, and scar location (Table 1).

Table 1 Patient demographic of selected scar samples

Group	*N*
All	18
Race	
Caucasian	6
Asian	12
Gender	
Male	12
Female	6
Age (years)	
<20	8
>20	10
Scar location	
Head and trunk	9
Upper extremities	3
Lower extremities	6
Scar ages	
1–5 months	7
6–10 months	6
>10 months	5

A total number of 18 skin lesions with typical contraction scar and surrounding unwounded skin between 1 and 12 months were matched according to patients' race, gender, age, scar location, and scar ages.

Animals

Male and female $Acta2^{+/+}$, $Acta2^{+/-}$, and $Acta2^{-/-}$ mice (10–12 weeks old and weighing from 18 to 23 g) were used in this study. The $Acta2^{-/-}$ mice used in this study were established by inserting the Pol2NeobpA cassette[15] into the +1 start site of the *Acta2* gene.[16] $Acta2^{-/-}$, $Acta2^{+/+}$, and $Acta2^{+-}$ mice from the same breeding colony were obtained from Warren E Zimmer, PhD at Texas A&M Health Science Center. All mice were monitored for signs of toxicity. The mice were housed under protocols approved by the Institutional Animal Care and Use Committee (IACUC) of Duke University.

Excisional Wounds and Gross Examination

All procedures were performed in accordance with a protocol approved by Duke University IACUC. Mice were anesthetized using gas anesthesia (oxygen, 2 l/min, isoflurane, 2%). The back of the mouse was shaved with metallic clippers. The back was then sterilized using alcohol. Full-thickness excisional wounds were created using 8-mm biopsy punches (Miltex, York, Gibbstown, PA, USA) in the area between mice's scapular angles. The wounds were then covered by Tegaderm (Transparent Film Dressing Frame Style, 3M Health Care, St Paul, MN, USA). Dressings were changed daily for the first 4 days and then removed. Wounds were measured and photographed daily using Canon PowerShot A470 digital camera. Wound contraction was measured by gravitational planimetry and expressed as percentage of original wound size.

Tissue Collection

Mice were euthanized and tissue was collected. Collected tissue was cut into equal halves. One half was preserved in 10% formalin for histological (HIS) analyses and the other half was immediately frozen in liquid nitrogen for additional analyses. Prior to staining, tissue sections were deparaffinized by warming at 65 °C overnight, immersed in xylene for 15 min, and rehydrated with decreasing concentrations of ethanol in distilled water.

HIS, Immunohistochemical, and Immunofluorescence Analysis

For HIS analysis, hematoxylin and eosin (H&E, Sigma-Aldrich, St Louis, MO, USA) staining was performed following standard techniques. Masson's Trichrome staining was performed by use of Trichrome Stain kit (Sigma-Aldrich), for collagen evaluation. The collagen index value was calculated as collagen index = B+G/2 R+B+G for each pixel within the image (where R, G, and B represent the red, blue, and green pixel values, respectively). The value of the collagen index ranged from 0 for extremely red objects to 1 for completely blue–green objects. The average collagen index of three (HPF) images for each time point was graphed.

For immunohistochemical (IHC) analysis, immunostaining was done. Briefly, to inhibit endogenous peroxidase activity, rehydrated sections were immersed in 3% hydrogen peroxide (H_2O_2) for 10 min to block endogenous peroxidase. Slides were rinsed with deionized water and then placed under retrieval solution (Target Retrieval Solution, Dako North America Carpinteria, CA, USA) in a water bath (98 °C) to unmask antigens. After further tris-buffered saline (TBS, TBS Automation Washing Buffer, Biocare Medical, Concord, CA, USA) rinsing, sections were treated with 10% goat serum (Normal Goat Serum, Vector Laboratories, Burlingame, CA, USA) for 1 h to block non-specific antibody binding. The primary antibody was incubated overnight at 4 °C. The primary antibodies used included (1) for human scar tissue IHC: rabbit anti ACTA2 polyclonal antibody (1:100 dilution, Abcam, Cambridge, MA, USA), mouse anti ACTB monoclonal antibody (1:5000 dilution, Abcam), mouse anti-ACTG1 monoclonal antibody (1:1000 dilution, Santa Cruz Biotechnology, Santa Cruz, CA, USA); and (2) for mice wound tissue IHC: rabbit anti-Ki67 monoclonal antibody (1:400 dilution, Thermo Scientific, Rockford, IL, USA), rabbit anti-CD31 polyclonal antibody (1:200 dilution, Abcam). After washing with TBS, the slides were incubated with appropriate secondary antibody. The secondary antibodies used were: biotinylated goat anti-rabbit IgG (1:200 dilution, Vector Laboratories), goat anti-mouse IgG (1:200 dilution, Vector Laboratories), and horse anti-mouse IgG (1:200 dilution, Vector Laboratories). The reactions were developed with an avidin–biotin complex reaction (Vector Laboratories).

For immunofluorescence analysis, Terminal deoxynucleotidyltransferase (TdT) dUTP nick-end labeling (TUNEL) staining was performed by using *in situ* Cell Death Detection POD kit (Roche, IN, USA) according to the manufacturer's instructions. 4′,6-diamidino-2-phenylindole (DAPI) counter stain was performed with Vectashield Mounting Medium (Vector Laboratories, Burlingame, CA, USA). Labeled cells were visualized by use of a Nikon eclipse E600 microscope and images were captured with a Nikon DXM 1200 digital camera under the same setting. Morphometric evaluations were done from sections through the center of wounds in order to obtain the maximum wound area for evaluation. Measurements of epidermal thickness,[17,18] collagen content,[19] positive immunostaining intensity,[20] and counting[21–23] were performed with NIH ImageJ software, and all the analyses were run as triplicates. To quantify non-muscle myosin II (isoform a, b, c, and ASMA) level of expression in scar *vs* normal tissues by immunochemical stained image analysis, the 24-bit RGB images per region (300 p.p.i.) were converted to 8-bit gray value images with pixel intensity values ranging from 0 (black) to 255 (white) using NIH ImageJ software. An 8×8 mm sample region containing both scar and normal tissue was selected for analysis. The sample image was divided into an 8×8 grid (each box = 1 mm^2). A mean pixel intensity value for each box was measured using ImageJ. The middle four columns were excluded from analysis since the area contains both scar and normal tissues. As a result, 16-sample pixel intensity values were each obtained for normal and scar tissue. Statistical analysis was performed using JMP software (SAS Institute ver. 7). The means of the two samples were compared via Student's *t*-test. Differences were considered to be statistically significant at values of $P < 0.01$.

Statistical Analysis

All data are presented as the mean and s.e.m. of three independent experiments. Statistical differences were determined using Student's *t*-test or one-way ANOVA with Bonferroni's *post hoc* test. The difference was considered significant when the *P*-value was 0.05 or less.

RESULTS

Expression of ACTA2, ACTB, and ACTG1 in Unwounded Human Skin and Human Contracture Scar

In unwounded skin, expression of ACTA2 was absent in the epidermis and dermal fibroblasts, but expression was detected in SM cells of blood vessels and skin appendages, whereas ACTB and ACTG1 were expressed both in the epidermis and all the dermis including dermal fibroblasts (Figure 1a, upper row) of unwounded skin. In contracted scar, the epidermis was thickened and flattened, and the appendages were missing. ACTA2 expression in scar epidermis was absent. The expression of ACTA2 in scar dermis was detected in vascular SM cells and in cells located in the nodular structure in the deeper layers of the scar. ACTB and ACTG1 expression in scar epidermis was present similar to that in the unwounded skin epidermis, and the expression in the scar dermis was increased in comparison with ACTA2 (Figure 1b, upper row). The overall expression of ACTA2, ACTB, and ACTG1 (Figure 1c) was found to be significantly increased in contracted scar tissue when compared with unwounded human skin tissue (1.8-fold for ACTA2, 2.5-fold for ACTB and ACTG1; $P \leq 0.01$). Variation caused by patients' race, gender, age, scar location, and staining intensity of ACTA2, ACTB, and ACTG1 in unwounded tissue and scar were detected and summarized (Table 2).

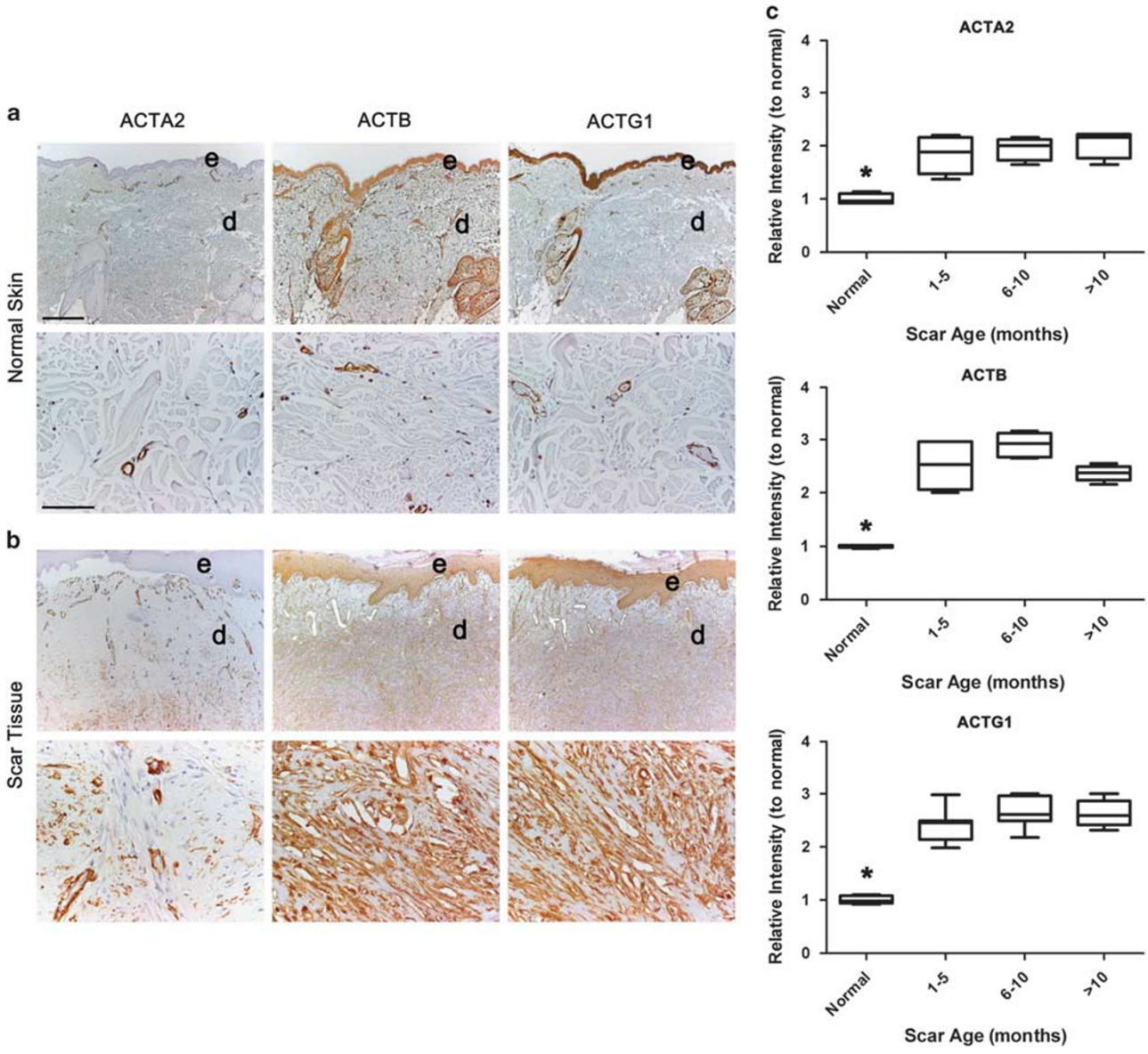

Figure 1 ACTA2, ACTB, and ACTG1 expression in the remodeling phase of repair. (**a**) Representative human unwounded skin. (**b**) Scar specimens investigated by IHC staining are shown to reveal the expression pattern of ACTA2, ACTB, and ACTG1. Scale bars, 400 μm for $\times 4$ (upper panel of (**a**) and (**b**)) and 100 μm for $\times 40$ (lower panel of (**a**) and (**b**)) images; e, epidermis; d, dermis. (**c**) The staining intensity of human unwounded skin tissue and contraction scar over time was quantified. Data are expressed as mean $\pm$ s.e.m. $^*P < 0.05$, tested by one-way ANOVA with Bonferroni's *post hoc* test, performed on 6- to 10-month *vs* >10-month scar for ACTB expression. ANOVA, analysis of variance; IHC, immunohistochemistry.

The Effect of ACTA2 Deficiency on Murine Wound Contraction

On day 2, compared with $Acta2^{+/-}$ mice ($85.5 \pm 1.9\%$), relative wound areas were significantly larger in $Acta2^{-/-}$ mice ($92.1 \pm 2.0\%$). There is no significant difference between $Acta2^{+/+}$ and $Acta2^{+/-}$ groups at days 3 and 4 after injury; however, the impaired wound contraction in $Acta2^{-/-}$ mice in comparison with that of $Acta2^{+/-}$ mice still presented significant difference afterwards except day 9. In comparison with the wound size of the $Acta2^{+/+}$ mice ($70.4 \pm 1.7\%$) the relative wound size on day 3 was significantly lager in $Acta2^{-/-}$ mice ($78.9 \pm 2.1\%$) and the delay in wound contraction in $Acta2^{-/-}$ mice group was observed up to day 11. Finally, 11 days after injury, the wounds of $Acta2^{-/-}$ mice healed to the same degree as those of $Acta2^{+/+}$ and $Acta2^{-/-}$ mice (Figure 2). Collectively, the gross wound contraction was delayed in the absence of ACTA2.

The Effect of ACTA2 Deficiency on Wound Evaluation

Microscopic assessment using H&E of wounds demonstrated that fibroblasts were the dominant cell type on days 7 and 11 in the wound area (Figure 3a). All the wounds in the mice

Table 2 ACTA2, ACTB, and ACTG1 expression comparison among groups

Group	*P*-value		
	ACTA2	ACTB	ACTG1
All	52.0 ± 1.7*	107.5 ± 3.7	104.3 ± 2.9*
Race			
Caucasian	49.5 ± 4.0	100.7 ± 7.7	98.2 ± 5.7
Asian	53.3 ± 1.6	110.8 ± 3.9	107.4 ± 3.0
Gender			
Male	51.6 ± 2.2	110.1 ± 4.5	103.6 ± 3.1
Female	52.8 ± 2.8	102.2 ± 6.5	105.8 ± 6.4
Age (years)			
<20	52.9 ± 1.9	111.7 ± 5.2	105.5 ± 4.1
>20	51.3 ± 2.7	104.1 ± 5.2	103.4 ± 4.2
Scar location			
Head and trunk	50.8 ± 4.5	103.7 ± 8.9	103.8 ± 6.9
Upper extremities	52.1 ± 3.2	114.6 ± 2.3	103.4 ± 9.1
Lower extremities	53.8 ± 2.2	109.5 ± 6.8	105.6 ± 4.1

Expression levels of ACTA2, ACTB, and ACTG1 in human contraction scar were measured by IHC staining intensity analysis. Values are indicated as mean ± s.e.m., for groups matched according to patients' race, gender, age, scar location, and scar ages, *$P<0.01$ tested by one-way ANOVA with Bonferroni's *post hoc* test, performed on ACTA2 *vs* ACTB, respectively. For groups matched according to tissue type, *$P<0.01$ tested by Student's *t*-test, performed on unwounded skin tissue *vs* scar tissue. ANOVA, analysis of variance; IHC, immunohistochemistry.

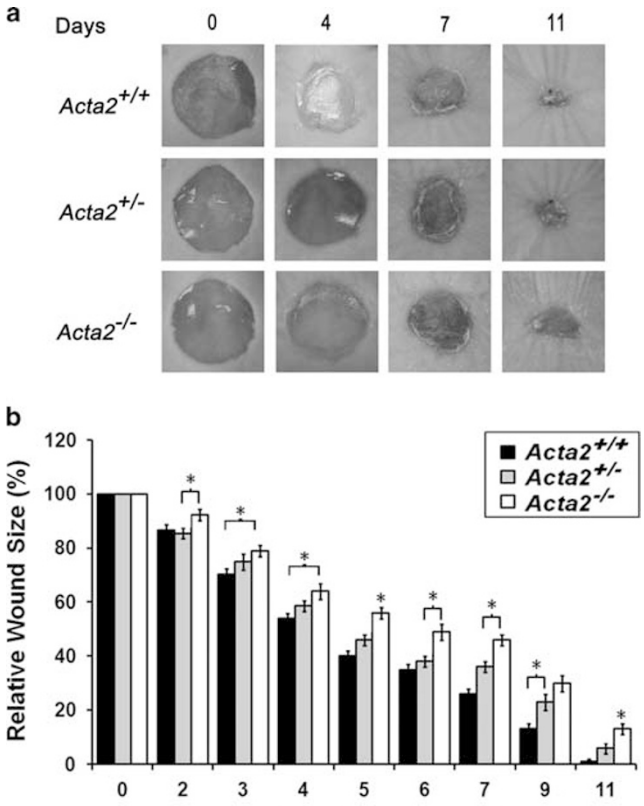

Figure 2 Skin wound healing of $Acta2^{+/+}$, $Acta2^{+/-}$, and $Acta2^{-/-}$ mice. (**a**) Representative macroscopic views from wounded mice are shown at days 0, 3, 7, and 11 post wounding. All pictures were taken at the same distance. (**b**) The fraction of wound area at indicated time point in comparison to the original wound area (quantified as described in Material and Methods section) was plotted and shown. Values are represented as mean ± s.e.m. ($n=25$, 31 and 38 for $Acta2^{+/+}$, $Acta2^{+/-}$, and $Acta2^{-/-}$ mice group). *$P<0.05$, tested by one-way ANOVA with Bonferroni's *post hoc* test, performed on $Acta2^{+/+}$ *vs* $Acta2^{+/-}$, $Acta2^{+/-}$ *vs* $Acta2^{-/-}$, and $Acta2^{+/+}$ *vs* $Acta2^{-/-}$, respectively. ANOVA, analysis of variance. A full color version of this figure is available at the *Laboratory Investigation* journal online.

were re-epithelialized by day 11. Increased numbers of fibroblasts were arranged in parallel to the epidermis and were observed in the scar area. Follicular sebaceous glands were present at the wound edge and juxtaposed unwounded tissue, but absent in the scar. The scar showed increased epidermal thickness compared to surrounding unwounded tissue (Figure 3b).

The Effect of ACTA2 Deficiency on Collagen Deposition in Wound Sites

Masson's Trichrome staining showed more collagen surrounding the fibroblasts in the granulation tissue area on day 11 compared to day 7 in all groups. Wounds in $Acta2^{+/-}$ and $Acta2^{-/-}$ mice showed scant collagen deposition (Figure 4a). Our analysis[19] has demonstrated a decrease in collagen accumulation in $Acta2^{+/-}$ and $Acta2^{-/-}$ mice compared to that observed in $Acta2^{+/+}$ mice (Figure 4b).

The Effect of ACTA2 Deficiency on Cellularity

To further assess the granulation tissue area in the different mice, Ki67, a nuclear antigen expressed in proliferating cells, was used to evaluate the proliferative activity of the fibroblastic area (Figure 5a). The number of Ki67-positive cells in the dermis of $Acta2^{-/-}$ mice wound was increased on days 7 and 11 compared to mice expressing ACTA2 (Figure 5b). Cellular apoptosis was assayed using TUNEL staining (Figure 6a), as apoptosis is a mechanism of myofibroblast resolution. The cellular apoptosis observed in the granulation tissue area of $Acta2^{-/-}$ mice was approximately half that compared to that observed in the granulation tissue area of $Acta2^{+/+}$ mice on days 7 and 11 (Figure 6b). DAPI staining was used to quantify cellularity. $Acta2^{-/-}$ mice had decreased number of cells in the granulation tissue area only on day 7 compared to that in mice expressing ACTA2 (Figure 6c). In summary, $ACTA2^{+/+}$ mice had a greater number of cells (as determined by DAPI) earlier in the wound

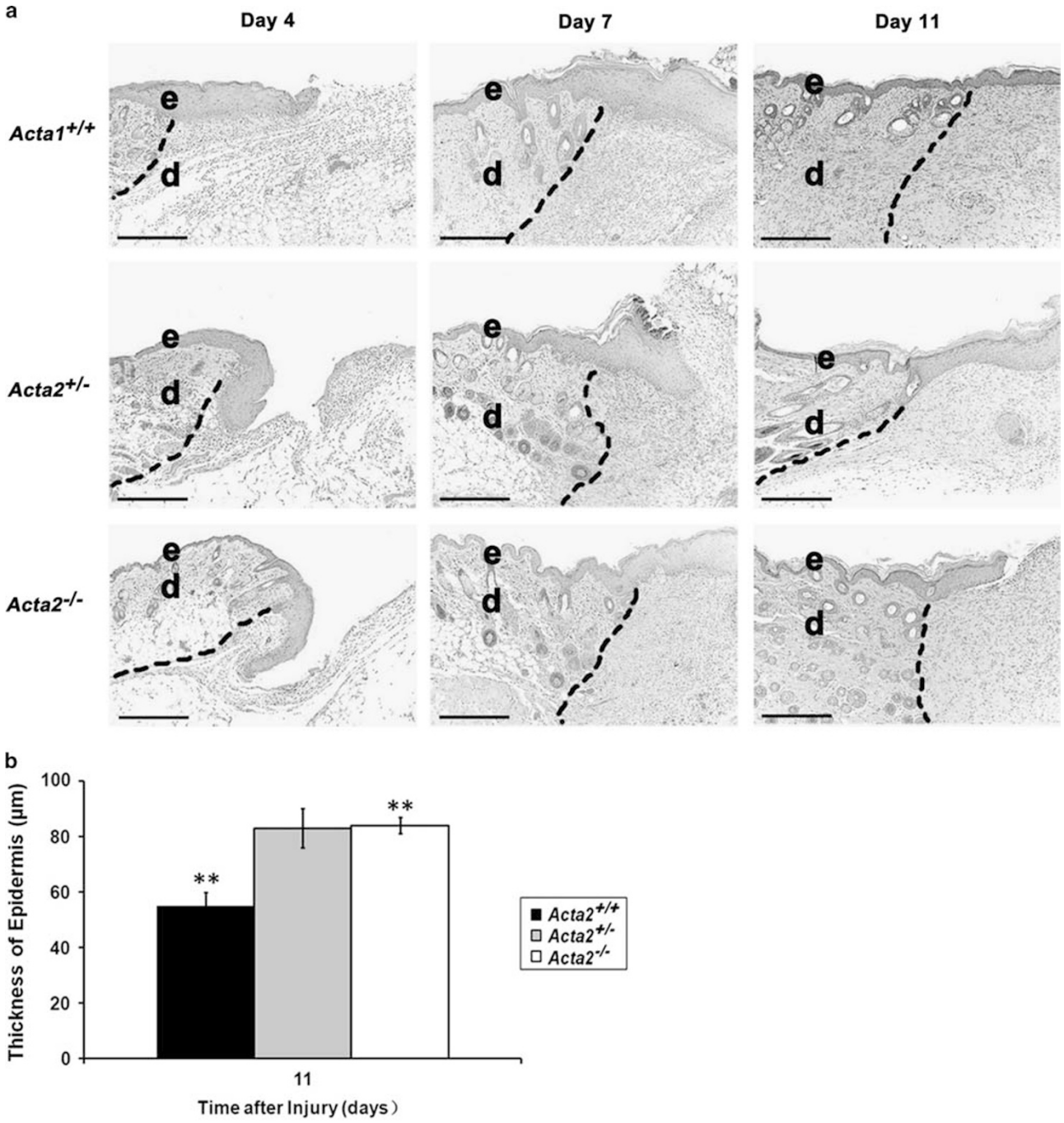

Figure 3 Histological evaluation of wounded skin. (**a**) H&E staining was performed at days 4, 7, and 11 after injury. Representative results from *Acta2*$^{+/+}$, *Acta2*$^{+/-}$, and *Acta2*$^{-/-}$ mice are shown. The dotted lines indicate the margin areas of the wound. Scale bars, 200 μm for $\times$10 images; e, epidermis; d, dermis. (**b**) Epidermal thickness was measured in *Acta2*$^{+/+}$, *Acta2*$^{+/-}$, and *Acta2*$^{-/-}$ mice at day 11 after injury. Data are expressed as mean $\pm$ s.e.m. ($n=3$ per genotype). $^{**}P<0.05$ tested by one-way ANOVA with Bonferroni's *post hoc* test, performed on *Acta2*$^{+/+}$ *vs* *Acta2*$^{+/-}$ and *Acta2*$^{+/+}$ *vs* *Acta2*$^{-/-}$, respectively. ANOVA, analysis of variance; H&E, hematoxylin and eosin. A full color version of this figure is available at the *Laboratory Investigation* journal online.

repair process; however, due to the increased proliferation and decreased apoptosis in ACTA2$^{+/-}$ and ACTA2$^{-/-}$ mice, as observed on day 7, and relative reduction of proliferation and increase in apoptosis in ACTA2$^{+/+}$ mice, as observed on day 7, the level of cellularity in ACTA2$^{+/-}$ and ACTA2$^{-/-}$ mice eventually equaled that of ACTA2$^{+/+}$ mice on day 11. These observations relate to wound size and may simply reflect the need to heal the wound.

Neovascularization in Acta2$^{-/-}$ Mice

To assess neovascularization, CD31 immunostaining was performed (Figure 7a). Neovascularization relies upon SM

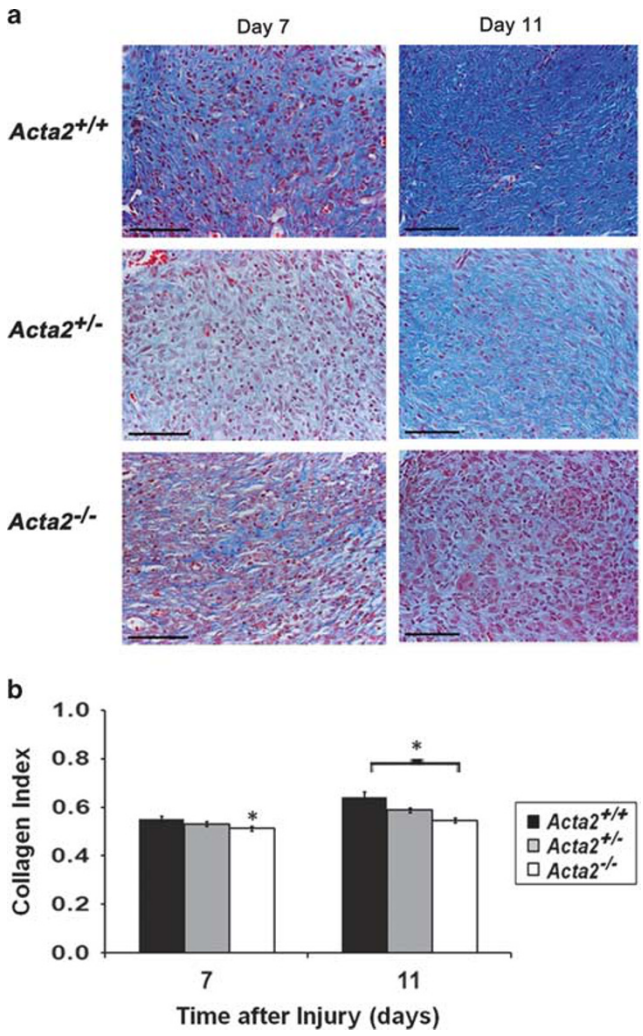

Figure 4 Representative wound section following Masson's Trichrome staining. (**a**) Collagen deposition and organization in days 7 and 11. Blue area represents collagen. (**b**) Collagen deposition results are shown as mean ± s.e.m. ($n = 3$ per genotype). *$P < 0.05$ tested by one-way ANOVA with Bonferroni's *post hoc* test, performed on $Acta2^{+/+}$ *vs* $Acta2^{-/-}$ for day 7 mice tissue, on $Acta2^{+/+}$ *vs* $Acta2^{+/-}$ and $Acta2^{+/+}$ *vs* $Acta2^{-/-}$ for day 11 mice tissue, respectively. Scale bars, 100 μm for ×40 images. ANOVA, analysis of variance.

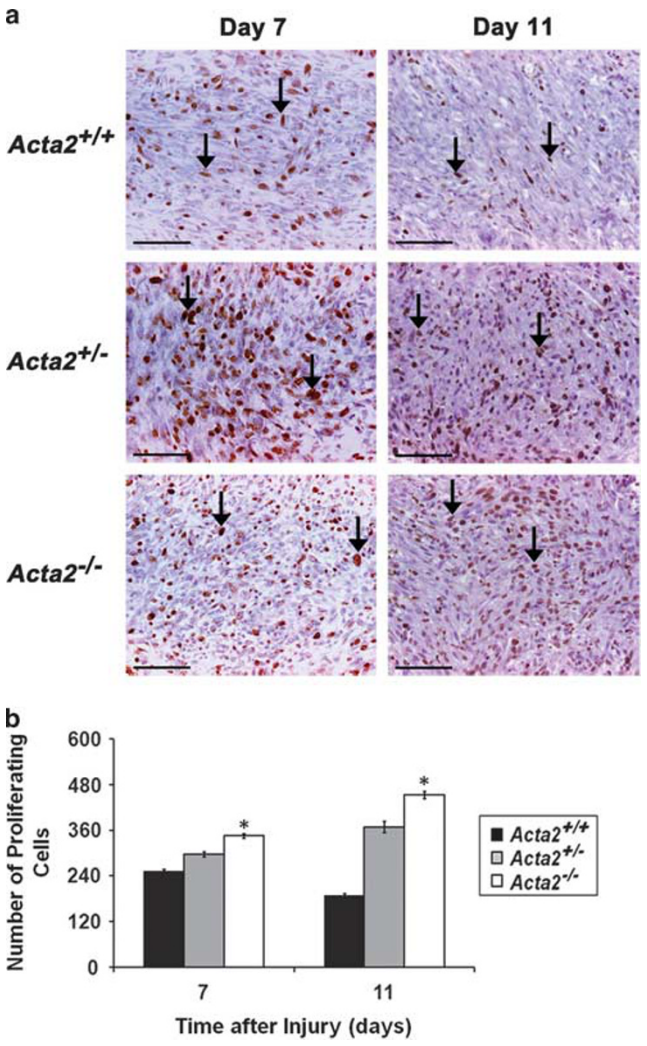

Figure 5 Proliferation activity in wound dermis. (**a**) Days 7 and 11 $Acta2^{+/+}$, $Acta2^{+/-}$, and $Acta2^{-/-}$ mice wound specimens were evaluated by staining with anti-Ki67 antibody. Representative photos are shown and Ki67-positive cells are indicated by black arrows. Level of cell proliferation was determined by the number of positive-stained nuclei in wound dermis. Scale bars, 100 μm for ×40 images. (**b**) Quantified data are represented as means ± s.e.m. ($n = 3$ per genotype). *$P < 0.01$ tested by one-way ANOVA with Bonferroni's *post hoc* test, performed on $Acta2^{+/+}$ *vs* $Acta2^{+/-}$, $Acta2^{+/-}$ *vs* $Acta2^{-/-}$, and $Acta2^{+/+}$ *vs* $Acta2^{-/-}$, respectively. ANOVA, analysis of variance.

cells, so mice deficient in ACTA2 could have defects in blood vessel formation that would affect healing. Compared to $Acta2^{+/+}$ mice, the granulation tissue areas of $Acta2^{+/-}$ and $Acta2^{-/-}$ mice had a surprisingly significantly greater number of vessels (Figure 7b). This result is consistent with previous mice wound contraction data and suggested that mice lack of ACTA2 expression have significantly enhanced level of angiogenesis than that of $Acta2^{+/+}$ mice.

DISCUSSION

In our current study, the use of $Acta2^{-/-}$ mice allowed us to directly test the role of alpha-SM actin-expressing myofibroblasts in wound contraction. Wound contraction started after surgery, and the contraction observed in $Acta2^{-/-}$ mice was significantly slower than that of $Acta2^{+/+}$ mice at all time points except day 2. The wound contraction difference between $Acta2^{+/+}$ and $Acta2^{-/-}$ mice peaked around day 7 post injury and then slowed down afterwards. Nonetheless, control mice healed their wounds. Collectively, these results identify a role for ACTA2 in wound closure but not an absolute necessity.

The wound healing process is a stepwise sequence of overlapping events, which often results in scar.[24] Persistent wound contraction after a wound has epithelialized leads to contractures, whereas delayed wound contraction leads to chronic non-healing wounds.[24] Current theories posit that

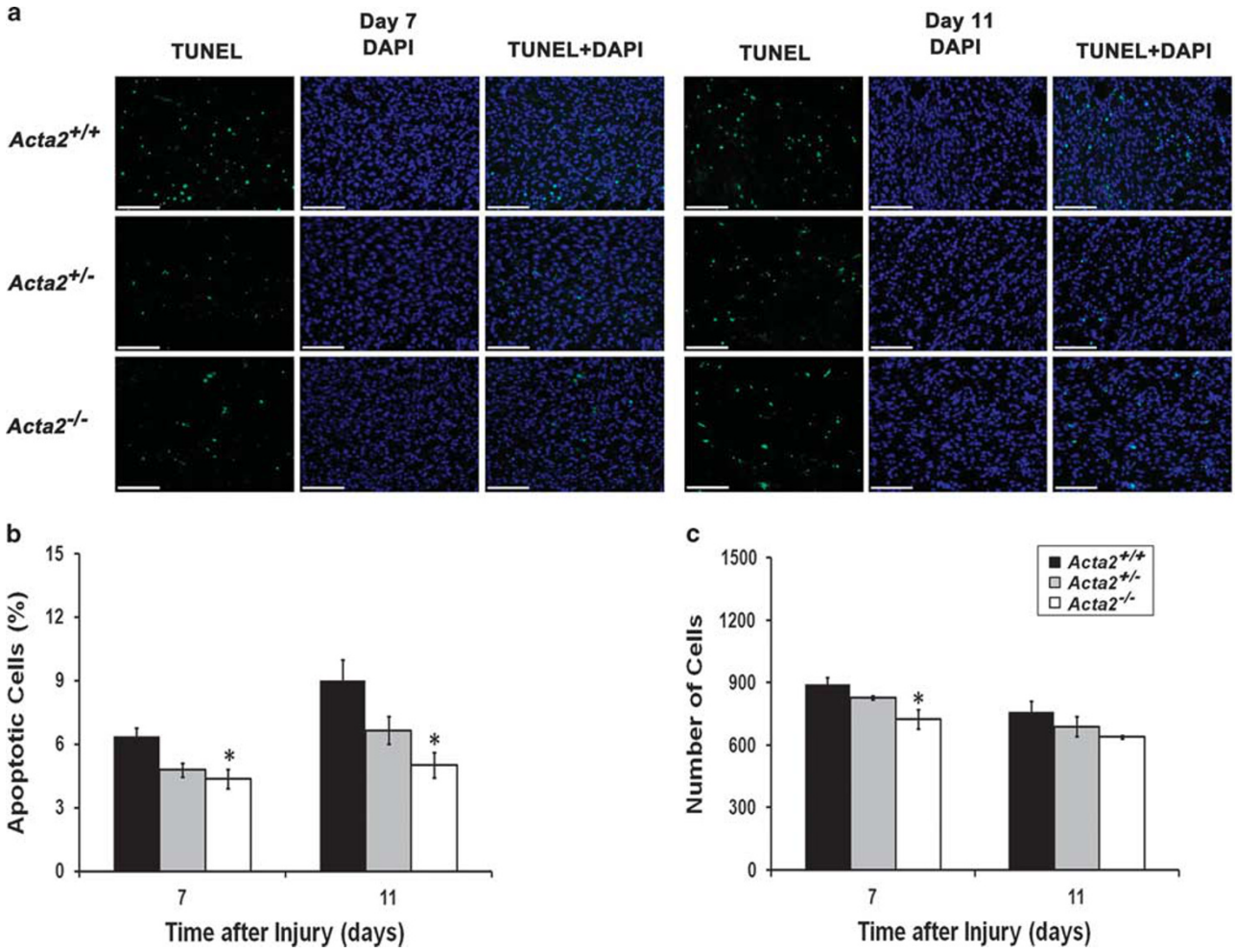

Figure 6 Apoptosis at wound sites. (**a**) TUNEL staining of wound sections were used for apoptosis detection (green), and DAPI staining was performed to visualize the total cell number (blue). Scale bars, 75μm for $\times 20$ images. Cell counting was performed at $\times 20$ magnification. Quantification of apoptosis ratio was achieved by plotting the number of TUNEL-positive cell against that of DAPI-positive cells (**b**). Wound cellularity was quantified by counting the number of DAPI-positive cells (**c**). Data are represented as means $\pm$ s.e.m. ($n = 3$ per genotype). *$P < 0.05$ tested by one-way ANOVA with Bonferroni's *post hoc* test, performed on *Acta2*$^{+/+}$ *vs Acta2*$^{-/-}$, respectively. ANOVA, analysis of variance; DAPI, 4',6-diamidino-2-phenylindole; TUNEL, terminal deoxynucleotidyltransferase (TdT) dUTP nick-end labeling.

alpha-SM actin-expressing myofibroblasts are necessary for wound contraction.[1] Although myofibroblasts are clearly present in granulation tissue during wound closure and in pathological contracture tissues, questions have arisen as to whether they are essential for collagen/granulation tissue contraction.[25] It is clear that traction forces that are generated by fibroblasts as they migrate on a compliant substratum can reorganize collagen matrices.[26] In fact, in free-floating collagen lattices the resulting reduction in lattice diameter is entirely due to fibroblast traction forces, which are generated by fibroblast migration and contractility.[27] This is sufficient to result in wound closure, this makes the involvement of a specialized contractile cell unnecessary.[9]

The gross evaluation from our study showed that the wound contraction rate of *Acta2*$^{-/-}$ mice do not match that of *Acta2*$^{+/+}$ and *Acta2*$^{+/-}$ mice but the wounds still contracted and closed. This actin expression defect disturbs the balance of wound contraction and regeneration, which sequentially upregulates the proportion of dermal regeneration in wound closure process.[28] As present results demonstrate, although *Acta2*$^{-/-}$ mice showed impaired wound contraction, they have increased neovascularization and cell proliferation in the wound bed as compared to *Acta2*$^{+/-}$ and *Acta2*$^{+/+}$ mice. The increase level of neovascularization in *Acta2*$^{-/-}$ mice implies that the absence of ACTA2 did not intervene the development and formation of new blood vessels, which complies with the previous finding of Ehrlich *et al*[12] that the development of ACTA2 in fibroblasts requires signals different from those required for these structures to appear in SM cells.

Wound contraction and scar contracture share a similar mechanism of action, namely, the contraction of the granulation bed.[3] Our current study started with IHC analysis of human contracture scar. Except blood vessels, ACTA2 was detected in the nodular structure found in contracture scar

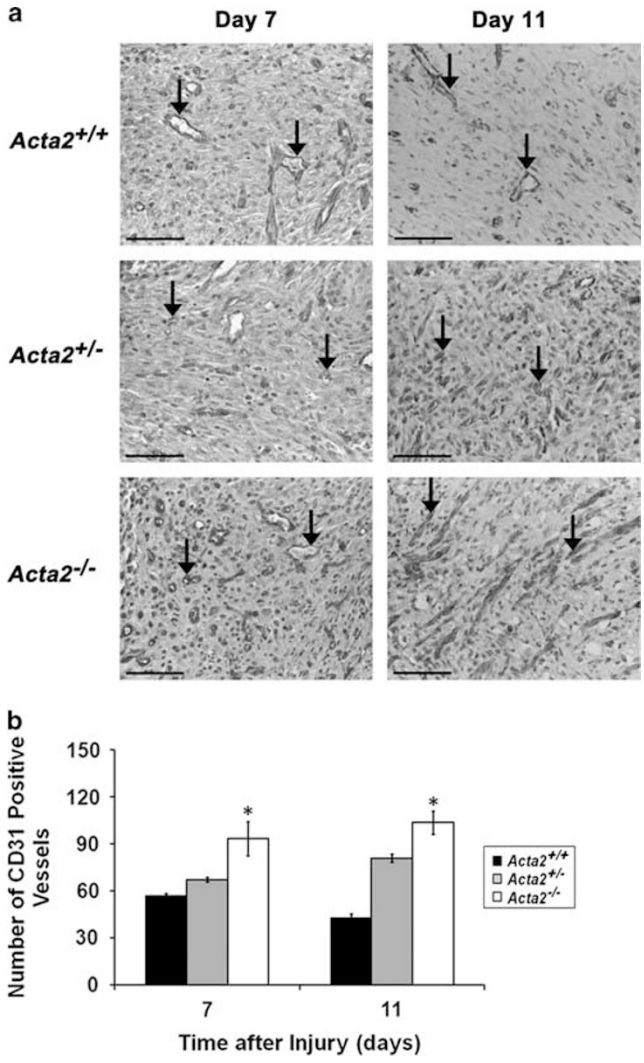

Figure 7 Angiogenesis in mice skin after wounding. (**a**) Days 7 and 11 $Acta2^{+/+}$, $Acta2^{+/-}$, and $Acta2^{-/-}$ mice wound sections were evaluated by staining with anti-CD31 antibody. Representative micrographs are shown and CD31-positive vessels were indicated by black arrows. Scale bars, 100 μm for $\times 40$ images. (**b**) Levels of vascularization were determined by the number of vessels stained positive for CD31 per high-power field in wound area. Data are represented as means $\pm$ s.e.m. ($n = 3$ per genotype). *$P < 0.05$ tested by one-way ANOVA with Bonferroni's *post hoc* test, performed on $Acta2^{+/+}$ *vs* $Acta2^{-/-}$ for day 7 mice tissue, on $Acta2^{+/+}$ *vs* $Acta2^{+/-}$, $Acta2^{+/-}$ *vs* $Acta2^{-/-}$, and $Acta2^{+/+}$ *vs* $Acta2^{-/-}$ for day 11 mice tissue, respectively. ANOVA, analysis of variance. A full color version of this figure is available at the *Laboratory Investigation* journal online.

samples, which is consistent with previous reports.[29,30] It appears that the existence of the particular nodule structure may have a relationship with the gross contractile characteristic of these samples.[30] The expression of ATCB and ACTG1 in the scar was significantly higher in comparison with that in unwounded tissue. In contrast with the local, nodular expression of ACTA2, ATCB, and ACTG1 was widely expressed throughout the scar. The proportional difference in actin isoform expression within scar brought up the same questions proposed by a sizeable body of studies[8,9,11,12,25,31–33] concerning the controversial role of ACTA2: (1) is the contribution of ACTA2 expression necessary for contractile force generation and tissue remodeling? (2) Will ACTB and ACTG1 expression sufficiently compensate the function of ACTA2?

In addition, there are variations in different investigations concerning the ACTA2 expression level in scar tissue.[29,30,34] Possible explanations for this inconsistency are: (1) differences in the sources of samples related with species, patients with demographic distribution; (2) differences in the samples' inclusion and exclusion criteria; (3) percentages of scar in different stages of repair process; (4) differences in the evaluation methods; and (5) sizes of sample population and observer variance. Our current research focuses on determining the relationship between actin isoforms and wound contraction. We observed a statistically significant higher expression of each actin in scar tissue, consistent with reports of Ehrlich *et al*,[30] our laboratories previous work,[20] Tian *et al*[35] and Wang *et al*.[34]

While our manuscript was in preparation, Tomasek *et al*[36] reported on wound healing in the $Acta2^{-/-}$ mouse. Analogous to our study, he found that ACTA2 expression was not necessary for wound closure. He reported that alpha-SM actin null fibroblasts become more contractile in response to TGF-β and that compensatory increases in actin isoforms, such as cardiac muscle α-actin, cytoplasmic β-actin, cytoplasmic γ-actin, skeletal muscle α-actin, and SM γ-actin could explain normal wound contraction rates. Differential expression of actin isoforms enabled non-alpha-SM actin isoform-expressing myofibroblasts to form. He also found a statistically different rate of wound contraction between animals, but not at all time points, as we observed. We believe that the discrepancies can be attributed to: (1) smaller wound sizes in his study, and (2) fewer time points to closure; meaning he may have missed statistically significant differences at more time points. Nevertheless, our work is in agreement with his that alpha-SM actin is not necessary for wound closure.

The present study has demonstrated that alpha-SM actin-expressing myofibroblasts contribute to but are not necessary for wound contraction. Although $Acta2^{-/-}$ mice showed impaired wound contraction, they have increased neovascularization and cell proliferation in the wound bed as compared to $Acta2^{+/-}$ and $Acta2^{+/+}$ mice. Compensatory increases in actin isoform expression may explain why wound contraction still occurs until wound closure. Thus, we posit that targeting contractile elements different than actin isoforms; yet, shared by myofibroblasts and fibroblasts (eg, non-muscle myosin II) may be a necessary approach for promoting healing of chronic wounds or reducing scar contractures.

Supplementary Information accompanies the paper on the Laboratory Investigation website (http://www.laboratoryinvestigation.org)

ACKNOWLEDGMENTS

This work was supported by a Plastic Surgery Foundation National Endowment Grant and by a grant from the National Institutes of Health K08GM085562. We thank Dr Bruce Klitzman for his supervision of animal experiment, Dr Zuowei Su for his advice and technical assistance for immunohistochemical experiments, Dr Luisa A DiPietro for her technical assistance, and Gloria Adcock for her assistance with tissue processing. We also thank Warren E Zimmer, PhD at Texas A&M Health Science Center for providing the ACTA2$^{-/-}$ mice used in this study and Dr Shaohai Qi for providing the human scar samples used in this work.

DISCLOSURE/CONFLICT OF INTEREST

The authors declare no conflict of interest.

1. Desmouliere A, Chaponnier C, Gabbiani G. Tissue repair, contraction, and the myofibroblast. Wound Repair Regen 2005;13:7–12.
2. Majno G, Gabbiani G, Hirschel BJ *et al.* Contraction of granulation tissue in vitro: similarity to smooth muscle. Science 1971;173:548–550.
3. Grinnell F. Fibroblasts, myofibroblasts, and wound contraction. J Cell Biol 1994;124:401–404.
4. Goffin JM, Pittet P, Csucs G *et al.* Focal adhesion size controls tension-dependent recruitment of alpha-smooth muscle actin to stress fibers. J Cell Biol 2006;172:259–268.
5. Hinz B, Dugina V, Ballestrem C *et al.* Alpha-smooth muscle actin is crucial for focal adhesion maturation in myofibroblasts. Mol Biol Cell 2003;14:2508–2519.
6. Darby I, Skalli O, Gabbiani G. Alpha-smooth muscle actin is transiently expressed by myofibroblasts during experimental wound healing. Lab Invest 1990;63:21–29.
7. Hinz B, Celetta G, Tomasek JJ *et al.* Alpha-smooth muscle actin expression upregulates fibroblast contractile activity. Mol Biol Cell 2001;12:2730–2741.
8. Berry DP, Harding KG, Stanton MR *et al.* Human wound contraction: collagen organization, fibroblasts, and myofibroblasts. Plast Reconstr Surg 1998;102:124–131.
9. Ehrlich HP, Rajaratnam JB. Cell locomotion forces versus cell contraction forces for collagen lattice contraction: an in vitro model of wound contraction. Tissue Cell 1990;22:407–417.
10. Ehrlich HP. Wound closure: evidence of cooperation between fibroblasts and collagen matrix. Eye 1988;2:149–157.
11. Ehrlich HP, Hembry RM. A comparative study of fibroblasts in healing freeze and burn injuries in rats. Am J Pathol 1984;117:218–224.
12. Ehrlich HP, Keefer KA, Myers RL *et al.* Vanadate and the absence of myofibroblasts in wound contraction. Arch Surg 1999;134:494–501.
13. Wrobel LK, Fray TR, Molloy JE *et al.* Contractility of single human dermal myofibroblasts and fibroblasts. Cell Motil Cytoskeleton 2002;52:82–90.
14. Martinez-Ferrer M, Afshar-Sherif AR, Uwamariya C *et al.* Dermal transforming growth factor-beta responsiveness mediates wound contraction and epithelial closure. Am J Pathol 2010;176:98–107.
15. Soriano P, Montgomery C, Geske R *et al.* Targeted disruption of the c-src proto-oncogene leads to osteopetrosis in mice. Cell 1991;64:693–702.
16. Rappolee DA, Mark D, Banda MJ *et al.* Wound macrophages express TGF-alpha and other growth factors in vivo: analysis by mRNA phenotyping. Science 1988;241:708–712.
17. Svensjo T, Pomahac B, Yao F *et al.* Accelerated healing of full-thickness skin wounds in a wet environment. Plast Reconstr Surg 2000;106:602–612.
18. Odland G, Ross R. Human wound repair. I. Epidermal regeneration. J Cell Biol 1968;39:135–151.
19. Olbrich KC, Meade R, Bruno W *et al.* Halofuginone inhibits collagen deposition in fibrous capsules around implants. Ann Plast Surg 2005;54:293–296.
20. Bond JE, Ho TQ, Selim MA *et al.* Temporal spatial expression and function of non-muscle myosin II isoforms IIA and IIB in scar remodeling. Lab Invest 2011;91:499–508.
21. Kyriakides TR, Wulsin D, Skokos EA *et al.* Mice that lack matrix metalloproteinase-9 display delayed wound healing associated with delayed reepithelization and disordered collagen fibrillogenesis. Matrix Biol 2009;28:65–73.
22. Javazon EH, Keswani SG, Badillo AT *et al.* Enhanced epithelial gap closure and increased angiogenesis in wounds of diabetic mice treated with adult murine bone marrow stromal progenitor cells. Wound Repair Regen 2007;15:350–359.
23. Di-Poi N, Ng CY, Tan NS *et al.* Epithelium-mesenchyme interactions control the activity of peroxisome proliferator-activated receptor beta/delta during hair follicle development. Mol Cell Biol 2005;25:1696–1712.
24. Lupher Jr. ML, Gallatin WM. Regulation of fibrosis by the immune system. Adv Immunol 2006;89:245–288.
25. Gross J, Farinelli W, Sadow P *et al.* On the mechanism of skin wound "contraction": a granulation tissue "knockout" with a normal phenotype. Proc Natl Acad Sci USA 1995;92:5982–5986.
26. Harris AK, Stopak D, Wild P. Fibroblast traction as a mechanism for collagen morphogenesis. Nature 1981;290:249–251.
27. Bell E, Ivarsson B, Merrill C. Production of a tissue-like structure by contraction of collagen lattices by human fibroblasts of different proliferative potential in vitro. Proc Natl Acad Sci USA 1979;76:1274–1278.
28. Yannas IV. Similarities and differences between induced organ regeneration in adults and early foetal regeneration. J R Soc Interface 2005;2:403–417.
29. Lee JY, Yang CC, Chao SC *et al.* Histopathological differential diagnosis of keloid and hypertrophic scar. Am J Dermatopathol 2004;26:379–384.
30. Ehrlich HP, Desmouliere A, Diegelmann RF *et al.* Morphological and immunochemical differences between keloid and hypertrophic scar. Am J Pathol 1994;145:105–113.
31. Ehrlich HP. Wound closure: evidence of cooperation between fibroblasts and collagen matrix. Eye (Lond) 1988;2:149–157.
32. Hembry RM, Bernanke DH, Hayashi K *et al.* Morphologic examination of mesenchymal cells in healing wounds of normal and tight skin mice. Am J Pathol 1986;125:81–89.
33. Bullard KM, Lund L, Mudgett JS *et al.* Impaired wound contraction in stromelysin-1-deficient mice. Ann Surg 1999;230:260–265.
34. Wang XQ, Kravchuk O, Winterford C *et al.* The correlation of in vivo burn scar contraction with the level of alpha-smooth muscle actin expression. Burns 2011;37:1367–1377.
35. Tian Y, Tang S, Luo S. A study on the expressions and the correlation of TGF-beta and alpha-SMA in scars. Zhonghua Zheng Xing Wai Ke Za Zhi 2000;16:75–77.
36. Tomasek JJ, Haaksma CJ, Schwartz RJ *et al.* Whole animal knockout of smooth muscle alpha-actin does not alter excisional wound healing or the fibroblast-to-myofibroblast transition. Wound Repair Regen 2013;21:166–176.